CHAPTER 110

A Model for Breaking Wave Impact Pressures

M.J. Cooker* and D.H. Peregrine†.

Abstract

This paper discusses a mathematical model of the large, short-lived pressures brought about by waves breaking against coastal structures. The idea of pressure impulse, P (the integral of pressure with respect to time from the start to the finish of the impact) is used to simplify the equations of ideal incompressible fluid notion. P satisfies Laplace's equation in a domain which is the mean position of the wave during the very short time of impact. We solve analytically a two-dimensional boundary-value problem, which models an idealized wave striking a vertical wall. Expressions are derived for the impulse on the wall, the peak pressure distribution, and the change in fluid velocity due to impact. The results are insensitive to the shape of the wave far from the wall. The results agree with some experimental measurements, from the literature.

Introduction

This paper is concerned with the very large and sudden pressures exerted by a breaking wave when it slams into a solid surface.

Winter storms in February 1990 caused great damage to sea walls on the UK coast, and there is a long-standing need to understand how breaking waves are able to exert loads on vertical walls, and other structures. Many field measurements and experimental studies since Bagnold (1939) have shown the existence of peak pressures exceeding 10 times the hydrostatic head and which last for periods between 0.1 and 10 milli-seconds (depending on the size of the wave). Figure 1 shows a typical pressure-time curve, for a point on a vertical wall. Blackmore and Hewson (1984) measured impact pressures in the field and high, short-lived loadings have been recorded on sloping beaches (Richert, 1968; Grüne, 1988).

----

*Research Assistant. †Professor.
School of Mathematics, University of Bristol, University Walk, Bristol, BS8 1TW, England.

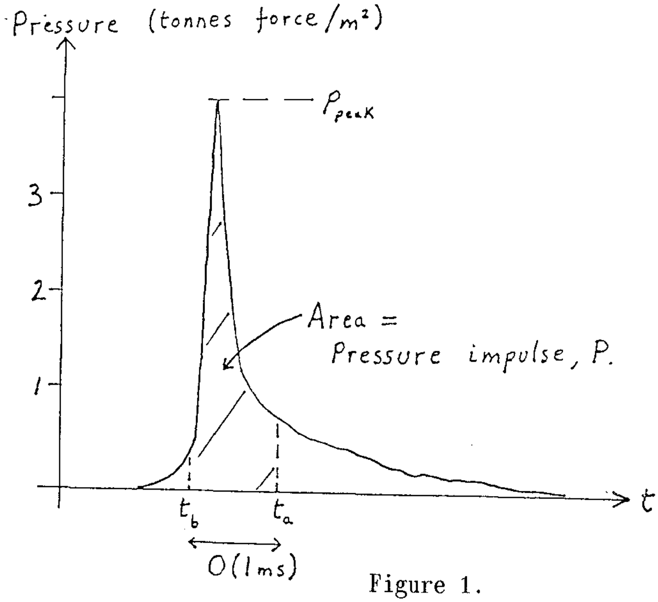

Figure 1.

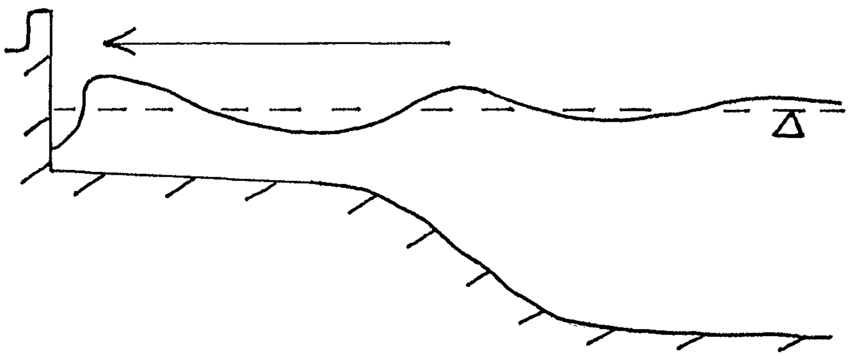

Figure 2. Sketch of wave steepening in shoaling water. A vertical face at the moment of impact, gives the highest peak impact pressures.

A full review of the literature is given by Cooker (1990, chap.6), and here we highlight the laboratory studies of Bagnold (1939), Nagai (1960) and Weggel and Maxwell (1970), all concerned with vertical walls. Current empirical engineering rules for peak pressure distribution p_{PK} at a vertical wall are summarized by Partenscky (1988). All these studies suggest that p_{PK} varies up and down the wall with a clear maximum near the water-line and a decrease toward the bed. Computations by Cooker and Peregrine (1990) reproduce these pressure distributions.

This paper puts these empirical rules on a rational basis by using the theory of pressure impulse, (Lagrange 1783),

$$P(x,y) = \int_{t_b}^{t_a} p(x,y,t)dt \qquad (1)$$

where t_b and t_a are the start and finish times of the impact. See figure 1.

Many experimenters have noted that under fixed wave conditions there is wide scatter in peak pressure. Bagnold (1939) pointed out that, despite the variations in p_{PK} (and in the impact time, $\Delta t \simeq$ twice pressure rise time), the product $p_{PK}\,\Delta t$ remains roughly constant;

$$P = p_{PK}\,\frac{\Delta t}{2} \qquad (2)$$

is an approximation to the definition of P in equation (1). Given the unavoidable difficulty of predicting p_{PK}, in this paper we suggest that pressure impulse is a more convenient concept, especially from a mathematical viewpoint. Below we show that P(x,y) satisfies Laplace's equation within a fluid domain which is the mean position of the fluid during the short time of impact. Armed with an analytic expression for P, and an estimate of the impact time Δt, we can use (2) to arrive at reasonable predictions for peak pressure distribution.

An advantage of this approach is that it allows us to model impact pressures due to even turbulent waves and, so far as P is concerned, the fluid can even be slightly aerated. The method can also be applied to more complex and three-dimensional wave impacts such as waves hitting a vertical cylinder. This is the subject of further work in progress.

Mathematical Model

We consider a wave in shoaling water approaching the shore from deeper water, and we expect typically the wave to steepen and break with a height possibly greater than the local still water depth, and with a speed greater than the maximum local wave speed

$(gh)^{\frac{1}{2}}$. Experiments show that the highest impact pressures occur when the wave face is vertical at the instant it strikes the wall. See figure 2.

We return to this specific problem below, but first consider a body of water striking a rigid surface. Let the impact speed be typically U_o, and the length-scale of the body of water be L_o. Let Δt be the impact time. Let U_o, L_o, Δt, p_o be independent velocity, length, time and pressure scales for the variables in Euler's equations, for two dimensional inviscid, incompressible flow. After some manipulation we arrive at an equation in dimensionless variables $\underset{\sim}{U}$, t, p, x, y

$$\frac{\partial \underset{\sim}{U}}{\partial t} + \frac{\Delta t U_o}{L_o} (\underset{\sim}{U} \cdot \nabla) \underset{\sim}{U} = \frac{-\Delta t p_o}{\rho U_o L_o} \nabla p \qquad (3)$$

where $\nabla = (\partial/\partial x,\ \partial/\partial y)$.

Typically $\Delta t U_o/L_o$ is very small ($\sim$0.03 in the computations of Cooker and Peregrine, 1990). The smallness of this dimensionless group enables us to discriminate between events which are "impact" and those which are not. If $\Delta t p_o/\rho U_o L$ is $O(1)$ then we have a balance between the first and last terms in equation (3), and the nonlinear 2nd term can be neglected.

We now integrate (3) with respect to time from $t = t_b$ to $t = t_a$, the duration of the impact. Returning to dimensional variables in (3) this gives us

$$\int_{t_b}^{t_a} \frac{\partial \underset{\sim}{U}}{\partial t}\, dt = \frac{-1}{\rho} \nabla \left\{ \int_{t_b}^{t_a} p\, dt \right\} .$$

From (1) this reduces to

$$\underset{\sim}{U}_a - \underset{\sim}{U}_b = \frac{-1}{\rho} \nabla P \qquad (4)$$

where $\underset{\sim}{U}_b$ and $\underset{\sim}{U}_a$ are the fluid velocities at times immediately <u>before</u> and <u>after</u> the impact, respectively.

We will also assume that the flow is incompressible so that both $\nabla \cdot \underset{\sim}{U}_b$ and $\nabla \cdot \underset{\sim}{U}_a$ vanish. Taking the divergence of (4) we arrive at Laplace's equation in the pressure impulse P

$$\nabla^2 P(x,y) = 0. \qquad (5)$$

Note that (5) does not involve time so we must solve boundary-value problems in a <u>fixed</u> domain which is a mean position for the fluid during impact. Finally note this theory admits arbitrary vorticity and can be extended to 3 dimensions.

Boundary-Value Problem.

Let us turn to the 2 dimensional problem in figure 3 for water wave impact on a vertical wall. Given $\underset{\sim}{U}_b$ we want to know $P(x,y)$ by solving (5) with appropriate boundary conditions, and then use (2) to find the peak pressure distribution. Also equation (4) gives us $\underset{\sim}{U}_a$, the flow immediately after impact; once we know P.

The boundary condition at the free surface is $P = 0$ because the pressure is a constant (zero) there. At the bed the vertical component of velocity $V = 0$ throughout the impact, so $V_a = V_b = 0$, hence from the vertical component of (4) we have $\partial P/\partial y = 0$. At the wall, we have chosen an upper region occupying a fraction of the wetted length, called the impact zone. Here the horizontal component of fluid velocity U changes from $U = U_b = -U_o$ before impact, to $U = 0$ after impact. From (4) this gives the boundary condition $\partial P/\partial x = -\rho U_o$ where $U_o > 0$ is a constant. Also $\partial P/\partial x = 0$ on the rest of the wall. Towards infinity $P \longrightarrow 0$. Figure 3 summarises the boundary value problem, and we can solve using Fourier analysis. A solution which satisfies the bed, free-surface and infinity boundary conditions is

$$P = \sum_{n=0}^{\infty} a_n \sin(\lambda_n y) e^{-\lambda_n x} \tag{6}$$

where $\lambda_n = (n+\frac{1}{2})\pi/H$.

The constants a_n are determined by the known values of $\partial P/\partial x$ at $x = 0$, the wall

$$\left.\frac{\partial P}{\partial x}\right|_{x=0} = \sum_{n=0}^{\infty} - a_n\lambda_n \sin \lambda_n y$$

$$\begin{pmatrix} = -\rho U_o & y: -\mu H \le y \le 0 \\ = 0 & y: -H \le y \le \mu H \end{pmatrix}$$

which give
$$a_n = \frac{-2\rho U_o}{H} \frac{(1-\cos\mu\lambda_n)}{\lambda_n^2} \tag{7}$$

and
$$P(x,y) = \frac{-2\rho U_o}{H} \sum_{n=0}^{\infty} \frac{(1-\cos\mu\lambda_n)}{\lambda_n^2} \sin(\lambda_n y)e^{-\lambda_n x}. \tag{8}$$

Note that for points $x > 0$ (away from the wall) the series in (8) is rapidly convergent because of the exponential terms. At the wall ($x = 0$) the distribution of pressure impulse is as shown in figure 4, for several values of μ.

Now from (2) we have

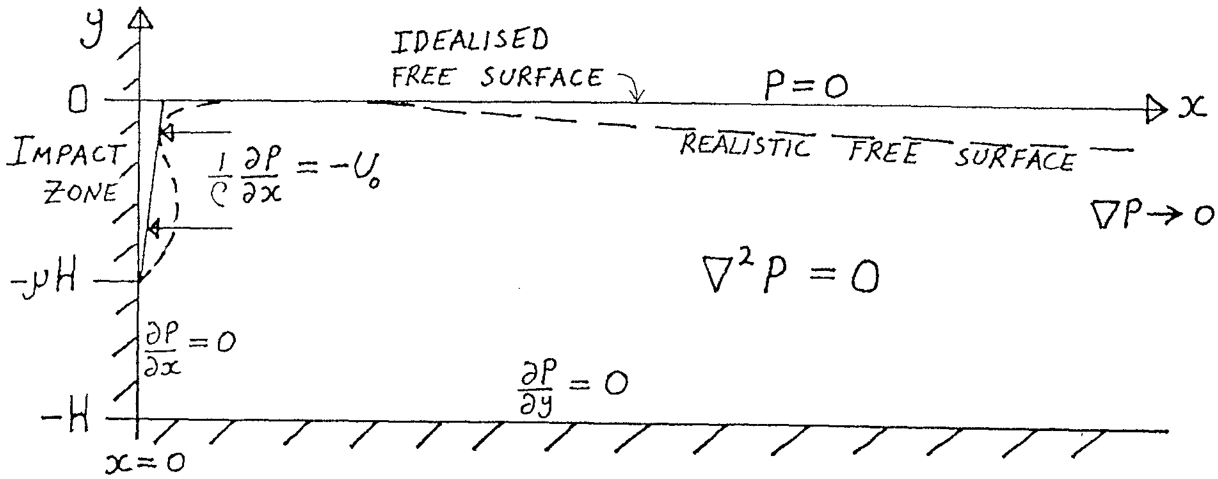

Figure 3. Semi-infinite rectangle geometry. Boundary-value problem for pressure impulse $P = \int_{t_b}^{t_a} p(x,y,t)\,dt$. Note the impact zone occupying the fraction μ of the wall.

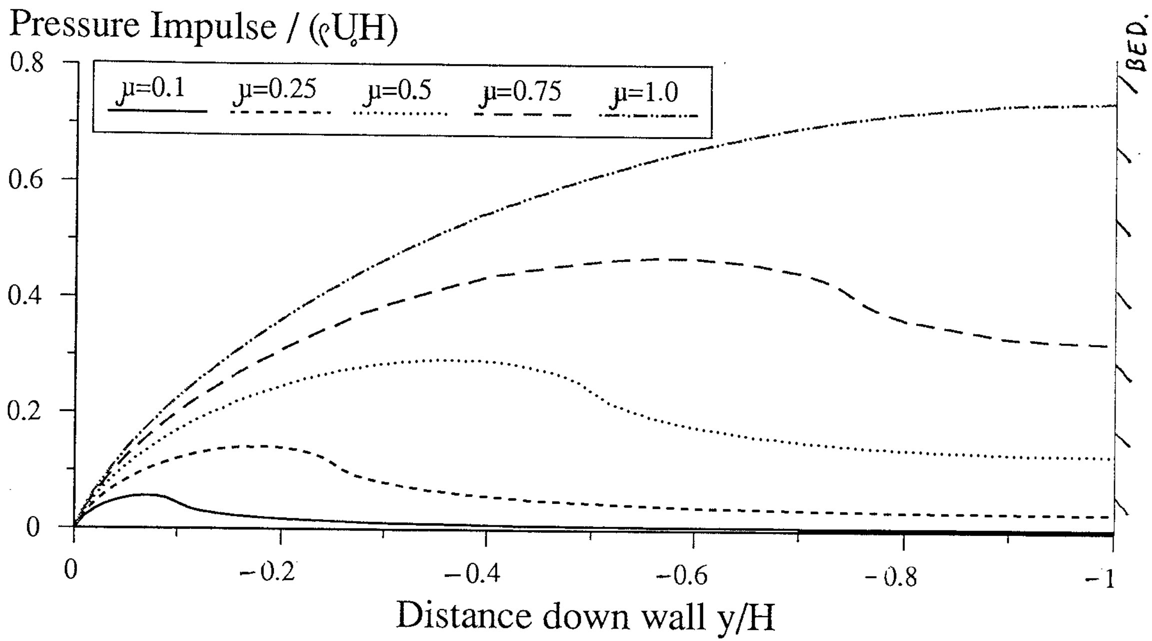

y=0 is the water-line, y/H=-1 is the bed.

Figure 4. Pressure impulse P from equation (3) at the wall (x = 0) for several values of μ. Note that P is directly proportional to the peak pressure.

$$p_{PK} = 2P/\Delta t \ .$$

The impact time, Δt, is difficult to model because it depends critically on the exact type of breaking at the wall, the air content of the fluid, and the inherent random qualities of impact under "fixed" wave conditions. Following experience from computations in Cooker and Peregrine 1990 it seems reasonable to take $\Delta t \propto \mu H$ e.g. $2\mu H/C_a$ where C_a is the sound speed in aerated water. The authors wish to make it clear that the above theory does not depend on any particular model or choice of Δt (so long as Δt is small, in the sense $\Delta t U_o/L_o << 1$). A designer may wish to use values of Δt gleaned from experience or which are related to the resonant frequency of the structure under wave attack.

The peak pressure distribution corresponding to a simple model: $\Delta t = \frac{1}{2}\mu H/U_o$ is shown in figure 5. Small values of μ are of particular interest, and the curves bear a striking resemblance to the empirical diagrams reported in Partenscky (1988). Note that the pressure does not decay to zero at the bed and that for $\mu = 1$ the maximum peak pressure lies at the bed.

The impulse on the whole wall, I_w, is the integral of (8) with respect to y, at x = 0, over the wall.

$$I_w = \frac{2\rho U_o}{H} \sum_{n=0}^{\infty} \frac{(1-\cos\mu\lambda_n)}{\lambda_n^3} \ . \tag{9}$$

See figure 6. In addition the impulse due to a finite triangular wave is shown. This result can also be found analytically. This comparison shows that the impulse is mainly due to the loss of momentum from fluid near the wall. We calculate the significant thickness of fluid L_m (momentum length) for the semi-infinite wave by equating I_w with the momentum of a rectangle of fluid of height μH, speed U_o, density ρ and length L_m. Then

$$L_m = \frac{2}{\mu H^2} \sum_{n=0}^{\infty} \frac{(1-\cos\mu\lambda_n)}{\lambda_n^3} \ . \tag{10}$$

Surprisingly L_m is at most 0.543H (when $\mu = 1$). This explains why the triangle and the infinite rectangle in figure 6 give impulses which are the same order of magnitude.

Last in this section of theoretical results we can use eq^n (4) to predict the fluid velocity after impact, $\underset{\sim}{U}_a$. This is most interesting to evaluate at the free surface. Suppose $V_b = 0$ (i.e. the top of the wave is in horizontal translation before impact) then taking the vertical component of (4) we have

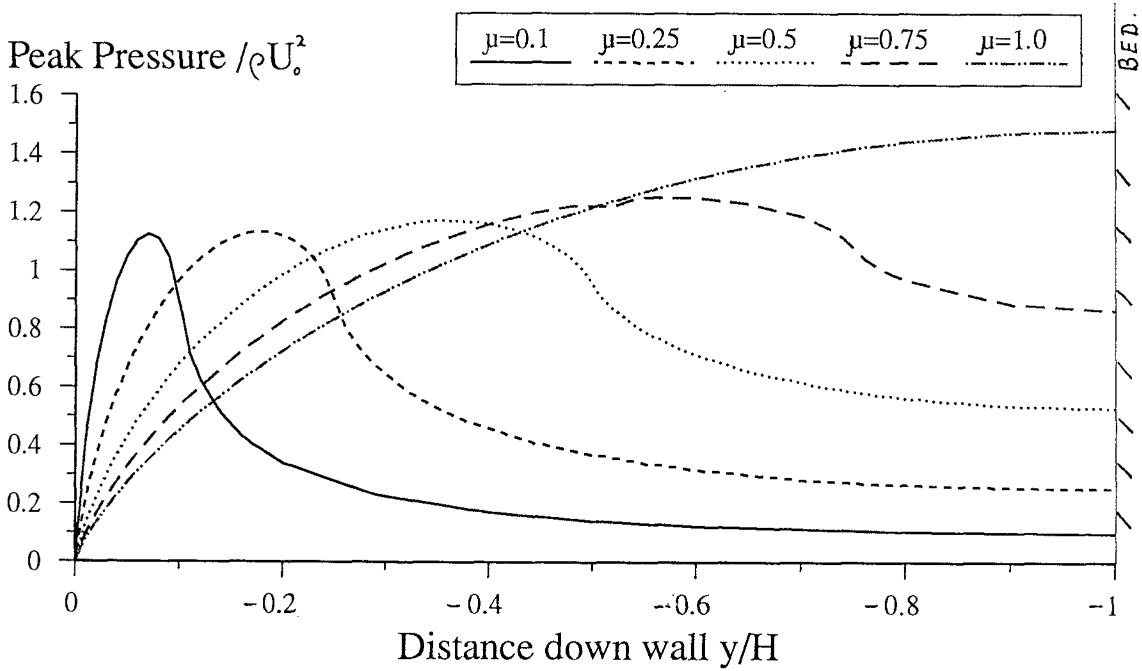

Figure 5. Peak pressure p_{PK} at the wall $p_{PK} = 2P/\Delta t$. Here Δt is modelled by $\frac{1}{2}\mu H/U_o$. Note the non-zero values of p_{PK} at the bed $(y/H = -1)$.

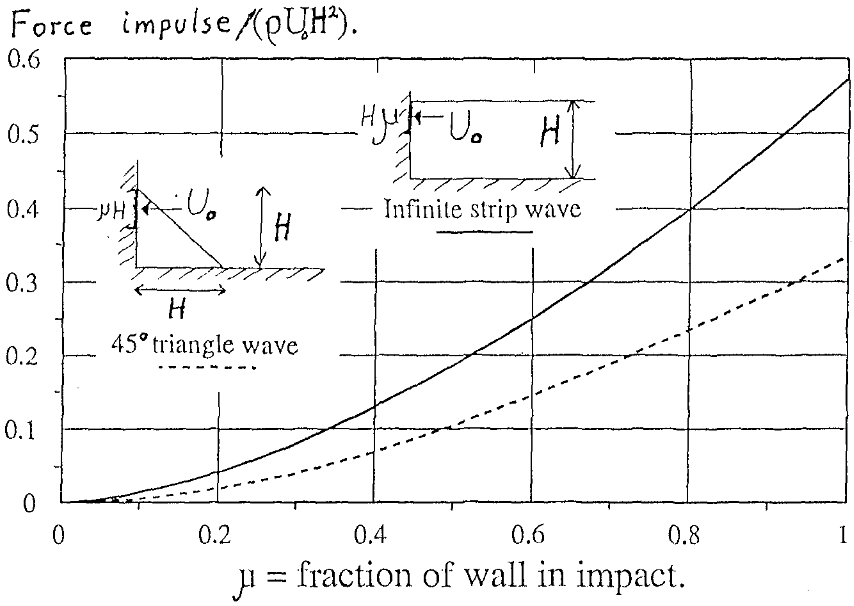

Figure 6. The impulse, I_w, on the wall from equation (9). The impulse due to a triangular wave (see sketch) is also plotted for comparison. The two waves are very different in shape but exert the same order of magnitude of impulse on the wall.

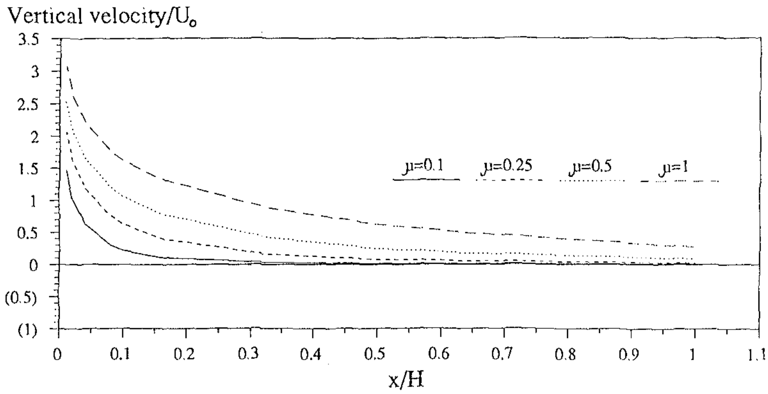

Figure 7. The vertical velocity at the free surface immediately after impact, V_a (with $V_b = 0$) from equation (11) Note these curves are proportional to surface elevation a small time after impact. The velocity near x = 0 resembles $\frac{-2U_o}{\pi}\ \ell n(x)$.

$$V_a \Big|_{y=0} = \frac{-1}{\rho}\frac{\partial P}{\partial y}\Big|_{y=0} = \frac{2U_o}{\Pi}\sum_{n=0}^{\infty}\frac{(1-\cos\mu\lambda_n)}{\lambda_n}e^{-\lambda_n x} \qquad (11)$$

$$= \frac{2U_o}{\pi}\ \ell n\left|\frac{\mathrm{cosech}\,\pi z/2+\coth\pi z/2}{\mathrm{cosech}\,\pi x/2+\coth\pi x/2}\right|$$

where $z = x + i\mu$.

At $x = 0$, V_a is infinite, but the vertical flux of fluid between $x = 0$ and any station $x = X$ is finite. V_a is plotted for several values of μ in figure 7. Note that the surface elevation, η, some small time T after impact is given by $\eta(x) = V_a(x)\cdot T$, so that the curves in figure 7 show possible *shapes* of the free surface after impact when the incident wave has a flat top, as in figure 2.

Comparison with Experiment

Figure 8 shows a comparison between the current theory and the peak pressure distributions for two small wave impacts, measured by Weggel and Maxwell (1970). Note that the pressure axis is dimensionless and that we are here comparing shapes of distribution of peak pressure. Our choice of μ accords with that chosen by the experimenters in their own mathematical model.

Figure 9 compares theory with large-scale experiments (Partenscky and Tounsi, (1989): peak values from figure 5). Here we have chosen $\mu = 0.24$, in agreement with the experimenters' choice for their comparison with theory. $H = 2.45$m, breaker height $= 1.5$m, so $U_o \simeq 3.8$ m/s. $\Delta t = 0.015$ (measured) which if $\Delta t = 2\mu H/C_a$ implies $C_a = 230$ m/s, (this corresponds to an air volume content of only 0.2%.

These comparisons encourage belief that pressure impulse theory captures the essential fluid mechanics of wave impact.

Conclusions

The theory of fluid pressure impulse has been used to model wave impact on a vertical wall. The results give spatial distributions of peak pressure which agree well with measurements. The theory predicts that the impulse on the wall is similar for two widely differing geometries (semi-infinite rectangle and 45° triangle). This is because the momentum lost from a wave of any shape comes from a narrow zone close to the wall (whose width is the momentum length). An important advantage of this theory is that it can be applied to waves with arbitrary vorticity. Further work is in progress to calculate pressure impulses due to three-dimensional waves.

References

Bagnold, R.A. (1939) Interim Report on Wave-Pressure Research. J.Inst. of Civil Engineers (1938-39), 12, p201-226.

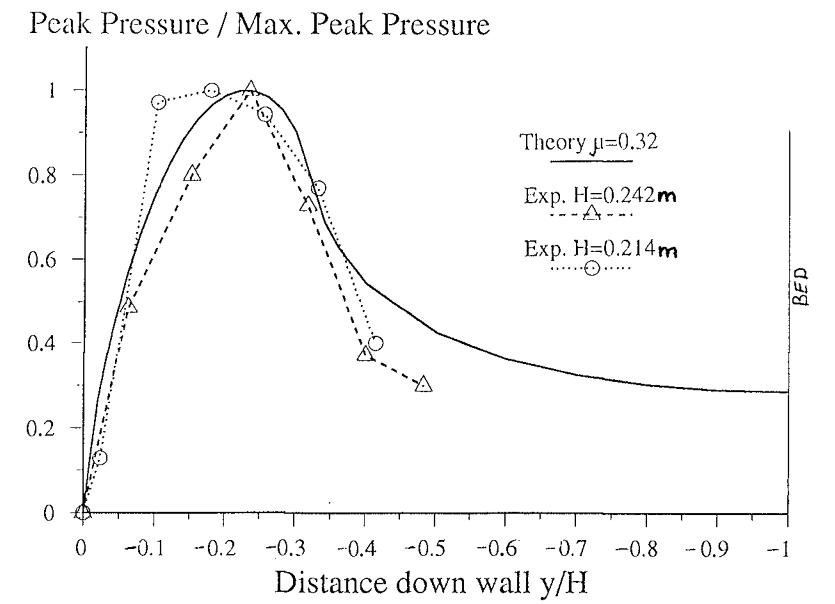

Figure 8. Comparison with experimental measurements of Weggel and Maxwell (1970), for two waves H = 0.242m and H = 0.214m. Note that the vertical scale is dimensionless and we have chosen μ = 0.32 in agreement with the experimenters' own numerical model.

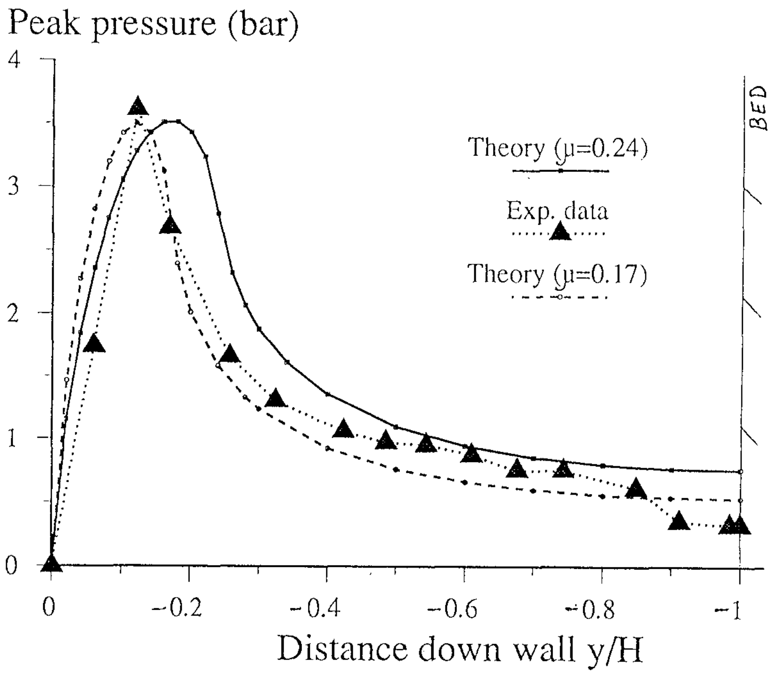

Figure 9. Comparison with experimental measurements of Partenscky and Tounsi (1989) (figure 5). $H = 2.45m$, $U = \sqrt{gH} = 4.9m/s$ and $\Delta t = 0.005s$. (The experimental data is the peak response at each recorder in the impact period). The theory with $\mu = 0.32$ is shown ($\mu = 0.32$ accords with the choice made by those authors for their numerical model). The present theory with $\mu = 0.17$ is also shown.

Blackmore, P.A. and Hewson, P.J. (1984) Experiments on full-scale wave impact pressures. Coastal Engineering (the journal), **8**, pp 331-346.

Cooker, M.J. (1990) The interaction between steep water waves and coastal structures. Ph.D. thesis, Univ. of Bristol, Apr. 1990.

Cooker, M.J. and Peregrine, D.H. (1990) Computations of violent motion due to waves breaking against a wall. 22nd Intl. Conf. on Coastal Engineering, Netherlands 1990, ASCE.

Grüne, J. (1988) Wave-induced shock pressures under real sea state conditions. 21st Coastal Eng. Conf., **3**, p2340-2354.

Lagrange, J.L. (1783) Memoire sur la théorie du mouvement des fluides, Nouv. Mem. de l'Acad. de Sci. de Berlin, **12**, p151-188.

Nagai, S. (1960) Shock pressures exerted by breaking waves on breakwaters. J. Waterways and Harbours Div. Proc., ASCE WW2, **86**, [SO-WW] pp1-38.

Partenscky, H.W. (1988) Dynamic forces due to breaking waves at vertical coastal structures. Proc. 21st Coastal Eng. Conf. June 1988, pp2504-2518.

Partenscky H.W. and Tounsi, K. (1989) Theoretical analysis of shock pressures caused by waves breaking at vertical structures. Intl. Assoc. for Hydraulic Research XXIII Congress, Ottawa, August 1989, 6 pages.

Richert, G. (1968) Experimental investigation of shock pressures against breakwaters. Proc. 11th Conf. Coastal Eng. ASCE, **1**, pp 954-973.

Weggel, J.R. and Maxwell, W.H.C. (1970) Numerical model for wave pressure distributions. J.W.H.O.E. Div. ASCE **96**, Aug. 1970, pp 623-642).